MOLECULAR AND CELLULAR BIOLOGY, June 1996, p. 3074–3084 Vol. 16, No. 6
0270-7306/96/$04.00+0

Insulin Signalling and Insulin Actions in the Muscles and Livers of Insulin-Resistant, Insulin Receptor Substrate 1-Deficient Mice

TOSHIMASA YAMAUCHI,[1] KAZUYUKI TOBE,[1] HIROYUKI TAMEMOTO,[1] KOHJIRO UEKI,[1] YASUSHI KABURAGI,[1] RITSUKO YAMAMOTO-HONDA,[1] YOSHIHIKO TAKAHASHI,[1] FUMIAKI YOSHIZAWA,[2] SHINICHI AIZAWA,[3] YASUO AKANUMA,[4] NAHUM SONENBERG,[5] YOSHIO YAZAKI,[1] AND TAKASHI KADOWAKI[1]*

Third Department of Internal Medicine, Faculty of Medicine, University of Tokyo, Tokyo 113,[1] Department of Science of Living, Iwate Prefectural Morioka Junior College, Morioka 020,[2] Laboratory of Morphogenesis, Institute of Molecular Embryology and Genetics, Kumamoto University School of Medicine, Kumamoto 860,[3] and The Institute for Diabetes Care and Research, Asahi Life Foundation, Tokyo 100,[4] Japan, and Department of Biochemistry, Faculty of Medicine, McGill University, Montreal, Quebec, Canada H3G 1Y6[5]

Received 5 February 1996/Returned for modification 13 March 1996/Accepted 25 March 1996

We and others recently generated mice with a targeted disruption of the insulin receptor substrate 1 (IRS-1) gene and demonstrated that they exhibited growth retardation and had resistance to the glucose-lowering effect of insulin. Insulin initiates its biological effects by activating at least two major signalling pathways, one involving phosphatidylinositol 3-kinase (PI3-kinase) and the other involving a ras/mitogen-activated protein kinase (MAP kinase) cascade. In this study, we investigated the roles of IRS-1 and IRS-2 in the biological actions in the physiological target organs of insulin by comparing the effects of insulin in wild-type and IRS-1-deficient mice. In muscles from IRS-1-deficient mice, the responses to insulin-induced PI3-kinase activation, glucose transport, p70 S6 kinase and MAP kinase activation, mRNA translation, and protein synthesis were significantly impaired compared with those in wild-type mice. Insulin-induced protein synthesis was both wortmannin sensitive and insensitive in wild-type and IRS-1-deficient mice. However, in another target organ, the liver, the responses to insulin-induced PI3-kinase and MAP kinase activation were not significantly reduced. The amount of tyrosine-phosphorylated IRS-2 (in IRS-1-deficient mice) was roughly equal to that of IRS-1 (in wild-type mice) in the liver, whereas it was only 20 to 30% of that of IRS-1 in the muscles. In conclusion, (i) IRS-1 plays central roles in two major biological actions of insulin in muscles, glucose transport and protein synthesis; (ii) the insulin resistance of IRS-1-deficient mice is mainly due to resistance in the muscles; and (iii) the degree of compensation for IRS-1 deficiency appears to be correlated with the amount of tyrosine-phosphorylated IRS-2 (in IRS-1-deficient mice) relative to that of IRS-1 (in wild-type mice).

Insulin induces a wide variety of growth and metabolic responses in many cell types. Insulin initiates its biological effects by activating tyrosine kinase in the β subunit (17) and phosphorylating several proteins (16, 39, 46, 49). These tyrosine-phosphorylated substrates bind several Src homology 2 proteins, thereby linking the tyrosine kinase to activation of at least two major signalling pathways, one involving a ras/mitogen-activated protein kinase (MAP kinase) cascade and the other involving phosphatidylinositol 3-kinase (PI3-kinase), which finally lead to insulin's biological actions.

Insulin receptor substrate 1 (IRS-1) is the major substrate of the insulin receptor kinase and has many tyrosine phosphorylation sites which provide binding sites for several distinct Src homology 2 proteins (e.g., Ash/Grb2 [abundant Src homology/growth factor receptor bound protein 2], the 85-kDa subunit of PI3-kinase [PI3-kinase p85], Syp, and Nck) and may mediate multiple signalling pathways (34, 45). In fact, IRS-1-deficient mice exhibited growth retardation and had resistance to the glucose-lowering effect(s) of insulin and insulin-like growth factor 1 (1, 36). However, the answer to the question of whether insulin resistance in IRS-1-deficient mice occurs at the level of liver and/or peripheral tissues, such as muscle and adipose tissue, is not clear, and it is not clear whether both the ras/MAP kinase pathway and the PI3-kinase pathway are affected.

When IRS-1 is tyrosine phosphorylated, it binds Ash/Grb2, thereby activating $p21^{ras}$ and leading to the activation of raf-1 kinase, MAP kinase kinase, MAP kinase, and p90 S6 kinase (MAP kinase cascade) (23, 33, 40). With regard to other IRSs, the transforming protein Shc (Src homology 2/α-collagen related) is also tyrosine phosphorylated and binds Ash/Grb2 (29, 49). Therefore, IRS-1 and Shc may constitute two major distinct pathways for insulin to activate a MAP kinase cascade through Ash/Grb2, although the relative contributions of these two pathways remain unclear and highly controversial. Several reports indicate that Shc was the predominant signalling molecule coupling insulin receptors to the activation of MAP kinase (31, 47). For example, in Rat1 fibroblasts overexpressing human insulin receptor, the majority of Ras guanylnucleotide exchange activity was found in Shc immunoprecipitates, with only a relatively small fraction being associated with IRS-1 immunoprecipitates (32). It has also been reported that overexpression of IRS-1 in Chinese hamster ovary cells expressing the mutant receptor which originally could not phosphorylate either IRS-1 or Shc restored IRS-1/Grb2 binding and yet MAP

* Corresponding author. Mailing address: Third Department of Internal Medicine, Faculty of Medicine, University of Tokyo, 7-3-1 Hongo, Bunkyo-ku, Tokyo 113, Japan. Phone: 81-3-3815-5411, ext. 3111. Fax: 81-3-5689-7209.

kinase activation was not rescued (4). However, the same group reported that expression of IRS-1 in 32-D cells caused a stimulation of MAP kinase by insulin through an enhancement of Grb2 binding to IRS-1 (24). The relative contributions of IRS-1 and Shc have not been determined in the physiological target organs in vivo.

When it is tyrosine phosphorylated, IRS-1 also binds PI3-kinase p85, thereby activating PI3-kinase (2, 18), leading to the activation of glucose transport into cells (3, 26), and p70 S6 kinase (3, 5). Since rapamycin, an immunosuppressant, completely inhibits the activation of p70 S6 kinase but has no effect on insulin-stimulated glucose transport in 3T3-L1 adipocytes (7), stimulation of glucose transport and activation of p70 S6 kinase by insulin seems to constitute two divergent pathways following the activation of PI3-kinase.

One of the downstream events in the activation of p70 S6 kinase and MAP kinase/p90 S6 kinase by insulin may be the stimulation of protein synthesis. The major effects of insulin are exerted at the initiation stage of translation. In this regard, insulin-stimulated activation of MAP kinase is thought to result in the increased phosphorylation of eukaryotic initiation factor 4E (eIF-4E)-binding protein 1 (4E-BP1), which then dissociates from eIF-4E, allowing the initiation of translation (20, 28). More recently, it has been shown that insulin promotes the phosphorylation of multiple sites in 4E-BP1 via multiple transduction pathways, one of which is likely to involve p70 S6 kinase, since it is rapamycin sensitive and independent of MAP kinase (9, 21). The phosphorylation of S6, which is also implicated in insulin-stimulated protein synthesis, most likely via an enhanced initiation of translation (13), is largely, if not exclusively, brought about by p70 S6 kinase rather than p90 S6 kinase (6, 30). In spite of the fact that insulin-stimulated protein synthesis is one of the major effects of insulin and that decreased protein synthesis in the muscle but not in the liver has been reported in diabetes (12), there has been no study reporting the role of IRS-1 in the control of mRNA translation and protein synthesis by insulin in muscle tissue.

IRS-2 is a substrate of insulin receptor kinase, has a molecular mass of approximately 190 kDa, has been identified in muscle and liver extracts, and can bind both PI3-kinase and Ash/Grb2 (1, 27, 41). Tyrosine phosphorylation of IRS-2 in IRS-1-deficient mice is significantly increased compared with that in wild-type mice. This increased level seems to compensate for IRS-1 deficiency at least in part and may partially rescue an otherwise much more severe insulin resistance in IRS-1-deficient mice. Recently, interleukin-4-induced phosphotyrosine substrate (4PS), which was originally found in interleukin-3-dependent myeloid cell lines as a common substrate for interleukin-4 receptor and insulin receptor kinase (43, 44), has been cloned (35) and reported to be the same molecule as IRS-2 (27). Although functional similarities between IRS-1 and IRS-2 have been suggested, primarily on the basis of their structural similarities, the biological functions of IRS-2 in the target organs of insulin are not known at present.

In this study, to evaluate the roles of IRS-1 and IRS-2 in insulin actions—especially the stimulation of glucose transport and protein synthesis, two major actions of insulin, in its physiological target organs—and to clarify the potential differences in the roles of IRS-1 and IRS-2 in different target organs, we investigated a variety of insulin signal transduction pathways in skeletal muscle and liver tissues from IRS-1-deficient mice. We also studied the tyrosine phosphorylation of IRS-2 in these target organs, especially in relation to the degree of insulin resistance. We show here that (i) the insulin resistance of IRS-1-deficient mice occurred at the level of skeletal muscles and was due to a decrease in the activation of PI3-kinase and glucose transport; (ii) IRS-1 also played an essential role in the activation of MAP kinase, p70 S6 kinase, and protein synthesis in the muscles; and (iii) the degree of compensation for IRS-1 deficiency appeared to be correlated with the amount of tyrosine-phosphorylated IRS-2 (in IRS-1-deficient mice) relative to that of IRS-1 (in wild-type mice).

MATERIALS AND METHODS

Mice and experimental design. The genotypes of the mice used were determined as described previously (36). Male mice weighing about 20 g (at 8 to 12 weeks of age) were used in these studies. They were starved overnight and anesthetized by the intraperitoneal administration of 100 μg of sodium pentobarbital per g of body weight 10 to 15 min before the experiment. For immunoblotting and the determination of PI-3 kinase and MAP kinase activity, skeletal muscles or livers were stimulated with insulin in vivo by an injection of the hormone via the portal vein. For determinations of the protein synthesis rate, glucose transport activity, and p70 S6 kinase activity, intact soleus muscles were excised and stimulated with insulin in vitro.

Antibodies. Monoclonal anti-phosphotyrosine antibody PY20, PY20 conjugated to alkaline phosphatase (RC20A), alkaline phosphatase-conjugated goat anti-mouse immunoglobulin G, and the polyclonal antibody against Shc were purchased from Transduction Laboratories. Rabbit polyclonal antibodies specific for phosphotyrosine were prepared as described previously (39). The monoclonal antibody against the 85-kDa subunit of PI3-kinase (AB6) was from MBL (Nagoya, Japan). The polyclonal antibody against Ash/Grb2 (C23) and the polyclonal antibody against the epitopes corresponding to residues 485 to 502 of rat p70 S6 kinase (C-18) were from Santa Cruz Biotechnology Inc. The polyclonal antibody (1-6) against a fusion protein of IRS-1 corresponding to residues 778 to 1243 (anti-IRS-1) was a kind gift from Masaki Nishiyama (Jikei University School of Medicine, Tokyo, Japan). The polyclonal antibody (179C) to IRS-2–4PS (anti-IRS-2) was raised against the peptide of DFLSHHLKEATVVKE, which corresponded to residues 1308 to 1322 of the amino acid sequence of mouse IRS-2 (35). The polyclonal antibodies to MAP kinase, αC92 and αY91, were raised against the peptide corresponding to residues 350 to 367 and 307 to 327 of extracellular signal-regulated kinase-1, respectively (38). The monoclonal antibody against eIF-4E, 10C6, and the rabbit polyclonal antibody against 4E-BP1 were generated as described previously (19, 28). A rabbit polyclonal antibody against a 20-amino-acid peptide with a sequence corresponding to the COOH-terminal sequence of glucose transporter 4 was from Hoffmann-La-Roche (Nutley, N.J.).

Materials. Porcine insulin was a gift from Eli Lilly Co. Actrapid human insulin was from Novo Nordisk A/S (Bagsvaerd, Denmark). Epidermal growth factor (EGF) was from Sigma. Wortmannin was kindly provided by Yuzuru Matsuda (Tokyo Research Laboratories, Kyowa Hakko Kogyo Co.). Phosphatidylinositol (bovine liver) was purchased from Avanti Polar Lipids, Inc. Protein G-Sepharose and 7-methyl-GTP (m^7GTP)–Sepharose were from Pharmacia Biotech Inc. All other materials were obtained from the sources described earlier (11).

Immunoblotting and PI3-kinase and MAP kinase assays. Immunoblotting and MAP kinase and PI3-kinase assays were performed as described previously (15, 37, 41). The portal vein was exposed, and 1 U of insulin per g of body weight or 500 ng of EGF per g body weight was injected via this vein. At the indicated time, the skeletal muscles from the hind limbs or the livers were removed, homogenized in ice-cold 1% Nonidet P-40–buffer A (25 mM Tris-HCl [pH 7.4], 10 mM sodium orthovanadate, 10 mM sodium PP_i, 100 mM sodium fluoride, 10 mM EDTA, 10 mM EGTA [ethylene glycol-bis(β-aminoethyl ether)-*N*,*N*,*N*′,N′-tetraacetic acid], and 1 mM phenylmethylsulfonyl fluoride), and centrifuged. Muscle homogenates containing 5 mg of total protein or liver homogenates containing 7.5 mg of total protein were incubated with the indicated antibodies, and then protein G-Sepharose was added. The immunoprecipitates were washed with 1% Nonidet P-40–buffer A three times. The immunoprecipitates were subjected to immunoblotting with RC20 followed by detection with the alkaline phosphatase conjugate system (Promega) or were probed with the indicated primary antibodies and then detected with ^{125}I-protein A (Amersham). The amount of tyrosine phosphorylation, normalized by the amount of receptor autophosphorylation, was evaluated by densitometry of the autoradiographs as described previously (4, 14).

The immunoprecipitates with PY20 were subjected to a PI 3-kinase assay, while those with αC92 were subjected to a MAP kinase assay. To 5 μl of the immunoprecipitates, 40 μl of kinase buffer (25 mM Tris-HCl [pH 7.4], 10 mM $MgCl_2$, 1 mM dithiothreitol, 40 μM ATP, 1 μCi of [γ-^{32}P]ATP [6,000 Ci/mmol; Du Pont NEN], 2 μM protein kinase inhibitor [rabbit sequence; Sigma], 0.5 mM EGTA) and 5 μl of myelin basic protein (MBP) (5 mg/ml) were added. After 15 min at 25°C, the reaction was stopped and the aliquots were spotted on squares of P81 paper (Whatman), washed, and counted by Cerenkov counting. Nonspecific ^{32}P incorporation was determined in identical assays lacking immune complex. In some experiments, the aliquots were not adsorbed to P81 paper and the reaction was stopped by the addition of 15 μl of 5× Laemmli buffer. The aliquots were subjected to sodium dodecyl sulfate-polyacrylamide gel electrophoresis

(SDS-PAGE) and then to autoradiography. The kinase assay in MBP-containing gel was performed as described previously (42).

Determination of the dissociation of the eIF-4E–4E-BP1 complex. We investigated the interaction between eIF-4E and 4E-BP1 as described previously (20, 21), with modifications. After a 10-min stimulation with insulin (1 U/g of body weight) or EGF (500 ng/g of body weight) via the portal vein, skeletal muscles from the hind limbs were removed, homogenized in ice-cold buffer B (1 mM EDTA, 5 mM EGTA, 10 mM $MgCl_2$, 2 mM dithiothreitol, 0.1 mM phenylmethylsulfonyl fluoride, 10 μg of leupeptin per ml, 10 μg of aprotinin per ml, 1 mM benzamidine, 10 mM KP_i, and 50 mM β-glycerophosphate [pH 7.3]), and centrifuged at 10,000 × *g* for 20 min. When m^7GTP-Sepharose was used, the homogenization buffer was 80 mM β-glycerol phosphate (pH 7.3)–50 mM NaF. We incubated the Sepharose with muscle extract (500 μl [5 mg of protein]) at 21°C, and after 30 min, the resin was washed three times with the same buffer before the proteins were eluted. When immunoprecipitation was done, the muscle extracts were incubated with 4E-BP1 antibodies (5 μg) coupled to protein G-Sepharose for 1 h at 4°C. The Sepharose was washed three times with buffer B before the proteins were eluted. For immunoblotting, the samples were probed with the monoclonal antibody against eIF-4E (diluted 2,000 times) or affinity-purified 4E-BP1 antibody (2 μg/ml), and the probing was followed by detection with alkaline phosphatase conjugated to goat anti-mouse immunoglobulin G or ^{125}I-protein A. The relative amounts of eIF-4E and 4E-BP1 were determined from the optical densities of the appropriate bands as described previously (9).

Determination of protein synthesis rate. The muscles used for the determination of protein synthesis were incubated as described previously (8, 50), with modifications. Briefly, soleus muscles isolated from the starved mice were preincubated with shaking at 110 oscillations per min for 30 min in 1 ml of Ham's F12 medium (Gibco). After the preincubation period, each muscle was incubated with shaking for 1 h in 1 ml of the same medium containing L-[2,3,5,6-^{3}H]tyrosine (5 μCi/ml; Amersham). To circumvent variations due to differences among animals, paired soleus muscles were used. Two paired soleus muscles were isolated from the same animal, with one muscle being incubated in the presence of 100 nM insulin or 100 nM EGF during the incubation and the other being used as a control without insulin. The gas phase in the flasks was 95% O_2–5% CO_2. At the end of the incubation, the muscles were freeze-clamped and homogenized in an ice-cold 10 mM Tris-HCl buffer (pH 7.5) containing 250 mM KCl, 10 mM $MgCl_2$, 6 mM 2-mercaptoethanol, and 0.1 mM phenylmethylsulfonyl fluoride. Homogenates were centrifuged at 12,000 × *g* for 30 min at 4°C. A 1-h time point had been shown to be within the linear range (data not shown). In some experiments, the protein synthesis rate was measured with or without a pretreatment with 50 nM wortmannin for 30 min. For the measurement of radioactivity in total soluble protein, the supernatants were spotted on Whatman 3MM paper strips and the strips were kept in boiling 10% trichloroacetic acid for 5 min, washed, and counted for radioactivity. The remaining portion of the supernatant was used to determine protein as described previously (22), with bovine serum albumin being used as a standard.

Measurement of glucose transport activity. This assay was performed as described previously (48), with modifications. Soleus muscles to be used for the measurement of insulin-stimulated glucose transport activity were placed in 2 ml of oxygenated Krebs-Henseleit bicarbonate (KHB) buffer containing 8 mM glucose, 32 mM mannitol, and 100 nM insulin and incubated with shaking at 110 oscillations per min at 35°C for 30 min. Control muscles were incubated under the same conditions without insulin. The gas phase in the flasks was 95% O_2–5% CO_2 throughout the experiment. After the initial incubation period, the muscles were transferred to flasks containing 2 ml of KHB buffer with 40 mM mannitol and incubated with shaking for 10 min at 29°C to remove glucose. Glucose transport activity was then measured with glucose analog 2-deoxy-D-glucose (2-DG). Osmolarity was kept constant throughout the experiment by varying the concentration of mannitol so that the sum of sugars equaled 40 mosM. Briefly, the muscles were incubated for 5 min at 29°C in 1.5 ml of KHB buffer containing 8 mM 2-deoxy-[1,2-^{3}H]glucose (2 μCi/ml; Du Pont NEN) and 32 mM [U-^{14}C]mannitol (0.1 μCi/ml; Du Pont NEN). After incubation, the muscles were blotted, frozen, weighed, homogenized in 1.5 ml of 10% trichloroacetic acid, and centrifuged at 1,000 × *g*. Duplicate aliquots of the supernatant were counted for radioactivity. The calculations of extracellular space and the 2-DG uptake rate were done as described above. The suitability of the use of 2-DG to measure hexose transport activity in isolated skeletal muscles has been reported (10). A 5-min time point had been shown to be within the linear range (data not shown). In some experiments, 2-DG uptake was measured with or without pretreatment with 50 nM wortmannin for 30 min by a protocol identical to that described above.

p70 S6 kinase activity in the immune complex. Briefly, isolated soleus muscles were incubated with shaking at 35°C for 30 min in KHB buffer containing 5 mM glucose and then were transferred to KHB buffer containing 5 mM glucose with or without 100 nM insulin or 100 nM EGF. The gas phase in the flasks was 95% O_2–5% CO_2. After 30 min, the incubations were terminated by freezing the muscles in liquid nitrogen. In some experiments, p70 S6 kinase activity was measured with or without pretreatment with 50 nM wortmannin for 30 min. The determination of p70 S6 kinase in the immune complex was performed as described previously (11).

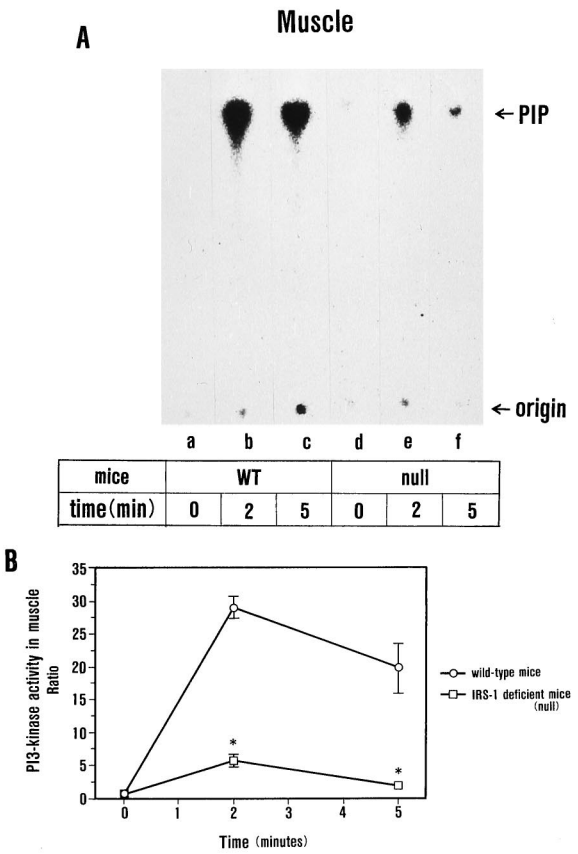

FIG. 1. PI3-kinase activity in the immunoprecipitates with αPY (anti-phosphotyrosine) from the muscles of wild-type (WT) and IRS-1-deficient (null) mice. The αPY (PY20) immunoprecipitates from the muscle extracts of untreated (time, 0 min) and insulin-treated wild-type and IRS-1-deficient mice for the indicated periods were subjected to a PI3-kinase assay. The autoradiogram of the thin-layer chromatograph is shown (A). The radioactivity in the spots corresponding to phosphatidylinositol (PIP) was measured, and the results, expressed as the ratios of the values for the respective mice to those for untreated and untreated wild-type mice, are shown (B). Each bar represents the mean ± standard error for muscles from five mice. *, $P < 0.001$ for insulin-injected wild-type mice versus insulin-injected IRS-1-deficient mice.

Statistical analysis. The results are presented as means ± standard errors of the means. The significance of the differences between the two groups was assessed by Student's unpaired *t* test.

RESULTS

PI3-kinase activity in skeletal muscles. We measured PI3-kinase activity in muscles from wild-type mice and IRS-1-deficient mice with the immunoprecipitates with the monoclonal antibody against phosphotyrosine (PY20). Two minutes after insulin injection, there was a maximal level of kinase activity (Fig. 1). In the muscles of wild-type mice, an insulin injection resulted in a 30-fold increase in PI3-kinase activity in PY20 immunoprecipitates, while in the muscles of IRS-1-deficient mice, it caused a 6-fold increase (Fig. 1). When the amounts of the 85-kDa subunit of PI3-kinase protein were assessed by immunoblotting with the monoclonal antibody against p85 (AB6), they were comparable for wild-type and IRS-1-deficient mice (data not shown).

Tyrosine phosphorylation of pp190 (IRS-2) is induced in the muscles of IRS-1-deficient mice, and pp190 can bind the 85-kDa subunit of PI3-kinase. Mice were injected with insulin, and 2 min after the injection, the phosphotyrosine proteins in

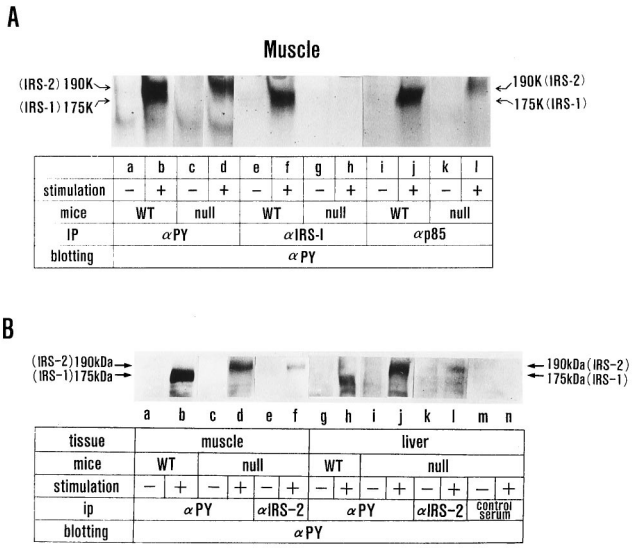

FIG. 2. Insulin-stimulated, tyrosine-phosphorylated proteins in the muscles and livers of wild-type and IRS-1-deficient mice. (A) PI3-kinase p85-associated, tyrosine-phosphorylated proteins in mouse muscles 2 min after insulin injection. (B) Identity of pp190 as IRS-2. Wild-type (WT) and IRS-1-deficient (null) mice were or were not injected with insulin via portal veins. After 2 min, the skeletal muscles from the hind limbs and the livers were removed, homogenized in 1% Nonidet P-40–buffer A (see Materials and Methods), and centrifuged. The supernatants were subjected to immunoprecipitation with αPY (PY20), αIRS-1 (1-6), αp85 (AB6), αIRS-2 (179C), or control rabbit preimmune serum and then to Western blotting (immunoblotting) with PY20 conjugated to alkaline phosphatase (RC20A). The results are representative of more than five separate experiments. IP or ip, immunoprecipitate; αPY, anti-phosphotyrosine.

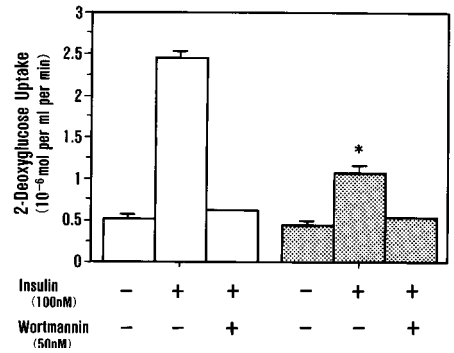

FIG. 3. Stimulation of 2-deoxy-[^{3}H]glucose uptake by insulin in soleus muscles from wild-type (open bars) and IRS-1-deficient (stippled bars) mice. Soleus muscles were incubated in oxygenated KHB buffer containing 8 mM glucose and 32 mM mannitol in the presence or absence of 100 nM insulin at 35°C for 30 min in a shaking incubator. The muscles were then transferred to KHB buffer containing 40 mM mannitol and washed for 10 min to remove glucose. The rate of 2-DG uptake was then measured as described in Materials and Methods. Each bar represents the mean ± standard error for 7 to 10 muscles without wortmannin. *, $P < 0.001$ for insulin-incubated muscles from wild-type mice versus insulin-incubated muscles from IRS-1-deficient mice. In some experiments, the rate of 2-DG uptake was measured after a pretreatment or not with 50 nM wortmannin for 30 min. The results for the muscles with wortmannin treatment are the means ± standard errors for two separate experiments shown in duplicate.

the muscles were determined by immunoblotting with PY20 conjugated to the alkaline phosphatase (RC20A) of PY20, anti-IRS-1 antibody (αIRS-1 [1-6]), anti-IRS-2–4PS antibody (αIRS-2 [179C]), and anti-p85 antibody (αp85) immunoprecipitates. We observed a 175-kDa tyrosine-phosphorylated protein in the muscles of insulin-injected wild-type mice (Fig. 2A, lane b). This 175-kDa tyrosine-phosphorylated protein was recognized by αIRS-1 and was thus identified as IRS-1 (Fig. 2A, lane f). In contrast, in IRS-1-deficient mice, although we did not observe tyrosine phosphorylation of IRS-1, we recognized a 190-kDa tyrosine-phosphorylated protein (pp190) in insulin-injected mice (Fig. 2A, lane d). The 190-kDa protein was not recognized by αIRS-1 (Fig. 2A, lane h) but was recognized by αIRS-2 and was thus identified as IRS-2–4PS (Fig. 2B, lane f). Next, we examined whether pp190 binds p85 as IRS-1 does. In αp85 immunoprecipitates of insulin-injected wild-type mice muscles, we observed a 175-kDa tyrosine-phosphorylated protein (Fig. 2A, lane j). In contrast, in insulin-injected IRS-1-deficient mice, a 190-kDa tyrosine-phosphorylated protein was present in αp85 immunoprecipitates (Fig. 2A, lane 1), indicating that pp190 bound the p85 of PI3-kinase in response to insulin. We previously reported that tyrosine phosphorylation of pp190 by insulin was significantly stimulated in the livers of IRS-1-deficient mice (41). The pp190 protein in liver tissue was also recognized by αIRS-2 and was thus identified as IRS-2–4PS (Fig. 2B, lane l). Immunoprecipitation of IRS-2–4PS is specific, because control rabbit preimmune serum did not recognize pp190 (Fig. 2B, lane n).

Glucose transport in skeletal muscles. We measured glucose transport activity in muscles from wild-type mice and IRS-1-deficient mice. Insulin (100 nM) stimulated the uptake of 2-DG into isolated soleus muscles from wild-type mice by about 4.8-fold, whereas it stimulated the uptake into muscles from IRS-1-deficient mice by only about 2.4-fold (Fig. 3). When the amounts of glucose transporter 4 protein were assessed by immunoblotting with the polyclonal antibody against glucose transporter 4, they were comparable in wild-type and IRS-1-deficient mice (data not shown). The glucose transport data (partial reduction in IRS-1-deficient mice) were consistent with the PI3-kinase data. To directly address whether the observed difference was indeed due to the PI3-kinase-dependent pathway, glucose transport activity was measured with pretreatment with 50 nM wortmannin, an inhibitor of PI3-kinase, for 30 min. Wortmannin almost completely prevented the increase in glucose transport activity in muscles from both wild-type and IRS-1-deficient mice exposed to insulin (Fig. 3).

p70 S6 kinase activity in skeletal muscles. It has recently been proposed that the activation of PI3-kinase may be upstream of p70 S6 kinase activation. Thus, to evaluate the role of IRS-1 and PI3-kinase in the activation of p70 S6 kinase in the target organs of insulin, intact soleus muscles were incubated in vitro with insulin and the p70 S6 kinase activity in muscles from wild-type and IRS-1-deficient mice was measured by immune complex assays. After a 30-min incubation, we observed a maximal increase in kinase activity under our conditions (data not shown). Insulin stimulation caused a 3.4-fold increase of p70 S6 kinase activity in the anti-p70 S6 kinase antibody (αp70 S6 kinase [C-18]) immunoprecipitates of muscles from the wild-type mice, whereas it caused a 1.6-fold increase in IRS-1-deficient mice (Fig. 4). Thus, consistent with the proposal discussed above, insulin-induced p70 S6 kinase activation was severely impaired, although not abolished, in skeletal muscles from IRS-1-deficient mice, and wortmannin almost completely abolished the insulin-stimulated increase in p70 S6 kinase activity (Fig. 4). When these mice were stimulated with EGF, which stimulates p70 S6 kinase via a pathway independent of IRS-1, the responses were comparable (data not shown). An assessment of the amount of p70 S6 kinase protein by immunoblotting with αp70 S6 kinase showed it to be comparable in wild-type and IRS-1-deficient mice (data not shown).

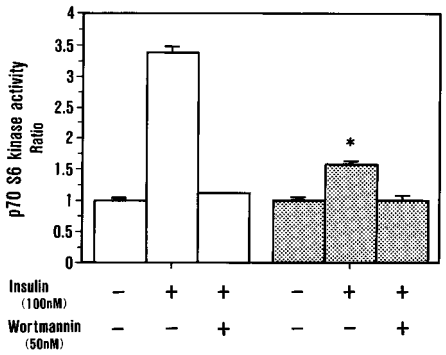

FIG. 4. p70 S6 kinase activity in the muscles of wild-type (open bars) and IRS-1-deficient (stippled bars) mice. Isolated soleus muscles from wild-type or IRS-1-deficient mice were preincubated for 30 min in KHB buffer containing 5 mM glucose and then were transferred to KHB buffer containing 5 mM glucose with or without 100 nM insulin. After 30 min, muscle extracts were prepared and then subjected to immunoprecipitation with the antibody against p70 S6 kinase (C-18). Immune complex kinase assays were performed as described in Materials and Methods. The results are expressed as the ratios of the values for the respective mice to those for untreated wild-type mice. Each bar represents the mean ± standard error for muscles from eight to nine mice without wortmannin treatment. *, $P < 0.001$ for insulin-incubated muscles from wild-type mice versus insulin-incubated muscles from IRS-1-deficient mice. In some experiments, the muscles were preincubated or not with 50 nM wortmannin for 30 min. The results for the muscles with wortmannin treatment are the means ± standard errors for two separate experiments shown in duplicate.

MAP kinase activity in skeletal muscles. To evaluate the relative roles of IRS-1–Grb2 complexes and Shc-Grb2 complexes in mediating the insulin stimulation of the MAP kinase cascade in insulin target organs in vivo, we measured MAP kinase activity in muscles from wild-type and IRS-1-deficient mice. There was a maximal increase in kinase activity 5 min after an insulin injection for both wild-type and IRS-1-deficient mice (Fig. 5A). Insulin stimulation caused a 3.4-fold increase of MAP kinase activity in the immunoprecipitates with the polyclonal antibody against MAP kinase (αC92) of muscles from the wild-type mice, whereas it caused a 1.7-fold increase in IRS-1-deficient mice. When these mice were stimulated with EGF, which stimulates MAP kinase via a pathway independent of IRS-1, the responses were virtually identical (about sixfold increases) (Fig. 5B), suggesting that the IRS-1-dependent pathway caused the difference in MAP kinase activation by insulin. When kinase assays were done in MBP-containing gels, the magnitude of the maximal MBP kinase activation in muscles from wild-type mice was also much greater than that in IRS-1-deficient mice (data not shown). The amounts of 42- and 44-kDa MAP kinase assessed by immunoblotting with the polyclonal antibodies against MAP kinase (αC92 and αY91) were comparable in the two groups (Fig. 5C and D).

Immunological detection of Ash/Grb2 associated with insulin-stimulated, tyrosine-phosphorylated proteins. Insulin causes the association of Ash/Grb2 with such phosphotyrosine-containing proteins as IRS-1 and Shc, and this association is involved in the activation of $p21^{ras}$ and the MAP kinase cascade. Five minutes after the injection, the Ash/Grb2-associated, phosphotyrosine-containing proteins in the muscles were determined by immunoblotting with the polyclonal anti-phosphotyrosine antibody of the anti-Ash/Grb2 antibody (αAsh/Grb2 [C23]) immunoprecipitates. In insulin-injected wild-type mouse muscles, we observed a 175-kDa tyrosine-phosphorylated protein (Fig. 6A, lane b), which was consistent with the

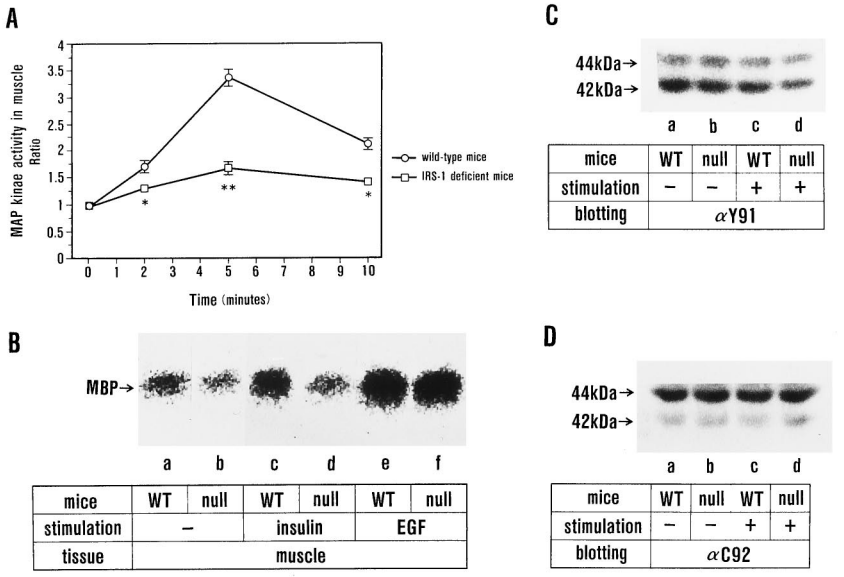

FIG. 5. MAP kinase activity in the muscles of wild-type (WT) and IRS-1-deficient (null) mice. (A) Time course of kinase activity of the immunoprecipitates with the antibody against MAP kinase (αC92) toward MBP. Muscle extracts from untreated (time, 0 min) and insulin-treated wild-type and IRS-1-deficient mice were subjected to immunoprecipitation with αC92 for the indicated time periods. The activity of MAP kinase was determined by incubation of the washed immunoprecipitates with MBP and [γ-^{32}P]ATP. Labeled MBP was spotted onto P81 phosphocellulose paper, and the paper was counted for radioactivity. The results are expressed as the ratios of the values for the respective mice to those for untreated wild-type mice. Each bar represents the mean ± standard error for muscles from 5 to 10 mice. *, $P < 0.01$; **, $P < 0.001$ (for wild-type versus IRS-1-deficient mice). (B) Insulin- or EGF-induced MAP kinase activity in the muscles of wild-type and IRS-1-deficient mice. Muscle extracts from untreated and insulin- or EGF-treated wild-type and IRS-1-deficient mice (treatment time, 5 min) were subjected to immunoprecipitation with αC92 and then to a kinase assay for MBP. Instead of being spotted onto P81 paper, labeled MBP was subjected to SDS-PAGE and then to autoradiography. The results are representative of five separate experiments. (C) Western blotting with the antibody against MAP kinase (αY91). Muscle extracts from untreated and insulin-treated wild-type and IRS-1-deficient mice (treatment time, 5 min) were subjected to SDS-PAGE and then to Western blotting with αY91. (D) Western blotting with αC92. Muscle extracts from untreated and insulin-treated wild-type and IRS-1-deficient mice (treatment time, 5 min) were subjected to SDS-PAGE and then to Western blotting with αC92.

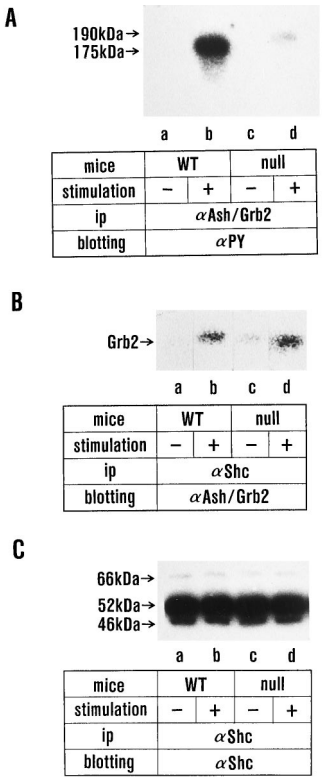

FIG. 6. Insulin-stimulated, tyrosine-phosphorylated proteins associated with Ash/Grb2 in muscles from wild-type and IRS-1-deficient mice. (A) Ash/Grb2-associated proteins in mouse muscles 5 min after insulin injection. The αAsh/Grb2 immunoprecipitates (ip) from the muscle lysates of wild-type (WT) (lanes a and b) and IRS-1-deficient (null) (lanes c and d) mice without (lanes a and c) and with (lanes b and d) insulin injection were subjected to Western blotting with the polyclonal anti-phosphotyrosine (αPY) antibody and then to detection with ^{125}I-protein A. The results are representative of five separate experiments. (B) Association of Shc with Ash/Grb2 in mouse muscles 5 min after insulin injection. The αShc immunoprecipitates from the muscle lysates of wild-type (lanes a and b) and IRS-1-deficient (lanes c and d) mice without (lanes a and c) and with (lanes b and d) insulin injection were subjected to Western blotting with αAsh/Grb2 and then to detection with ^{125}I-protein A. The results are representative of three separate experiments. (C) Amounts of Shc in muscles from wild-type and IRS-1-deficient mice. The αShc immunoprecipitates from the muscle lysates of untreated and insulin-treated wild-type and IRS-1-deficient mice (treatment time, 5 min) were subjected to Western blotting with αShc.

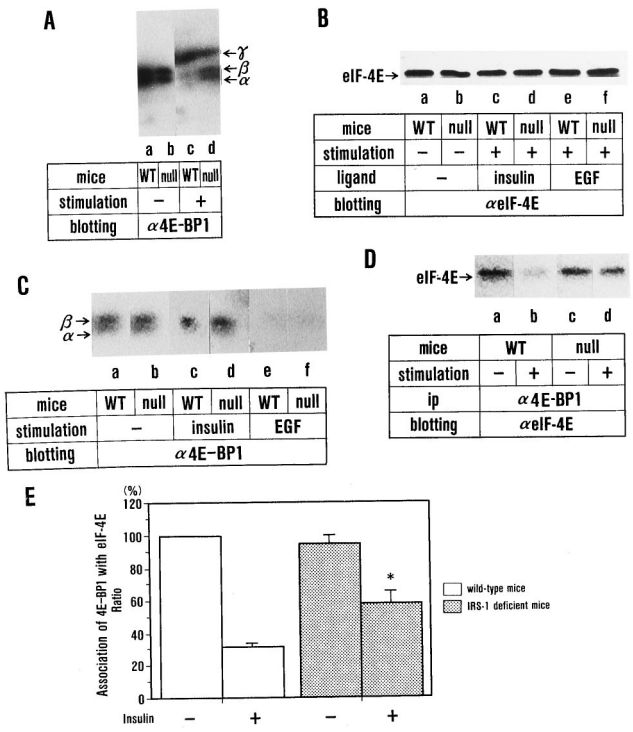

FIG. 7. Effects of insulin and EGF on the eIF-4E–4E-BP1 complex in muscles from wild-type (WT) and IRS-1-deficient (null) mice. Muscle extract samples from untreated and insulin-treated and EGF-treated wild-type and IRS-1-deficient mice (treatment time, 10 min) were subjected to SDS-PAGE, and 4E-BP1 was identified by immunoblot analysis with 4E-BP1 antibody (A). Other samples incubated with m^{7}GTP-Sepharose or 4E-BP1 antibody coupled to protein G-Sepharose were subjected to SDS-PAGE, and eIF-4E that was purified with m^{7}GTP (B), 4E-BP1 that was copurified with eIF-4E (C), and eIF-4E that was coimmunoprecipitated with the 4E-BP1 antibody (D) were identified by immunoblot analysis. The results are representative of more than three separate experiments. (E) The relative amounts of 4E-BP1 recovered with m^{7}GTP-Sepharose were determined from the optical densities of the appropriate bands on 4E-BP1 immunoblots. The results are expressed as percentages of the amounts of 4E-BP1 recovered from the muscles of untreated wild-type mice and are means ± standard errors for four independent experiments. *, $P < 0.05$ for insulin-injected wild-type mice versus insulin-injected IRS-1-deficient mice.

previous finding that Ash/Grb2 binds tyrosine-phosphorylated IRS-1. In insulin-injected IRS-1-deficient mice, however, we observed a 190-kDa tyrosine-phosphorylated protein in αAsh/Grb2 immunoprecipitates (Fig. 6A, lane d). Five minutes after the insulin injection, the association of Shc with Ash/Grb2 in the muscles was assessed by immunoblotting with the antibody against Ash/Grb2 of the anti-Shc antibody (αShc) immunoprecipitates. Shc could bind Ash/Grb2 in the muscles of IRS-1-deficient mice to the same extent as it could in those of wild-type mice (Fig. 6B, lanes a to d). Occasionally, the association of Shc with Ash/Grb2 was increased slightly but not significantly. When the amounts of Shc proteins were assessed by immunoblotting with the polyclonal antibody against Shc of the αShc immunoprecipitates, they were comparable in wild-type and IRS-1-deficient mice (Fig. 6C). Under our conditions, we were unable to separate the 52-kDa Shc isoform from the background staining of the immunoglobulin G heavy chains.

Dissociation of the eIF-4E–4E-BP1 complex in skeletal muscles in vivo. To evaluate the role of IRS-1 in mediating the insulin stimulation of mRNA translation in insulin target organs in vivo, we investigated the phosphorylation of 4E-BP1 and the dissociation of the eIF-4E–4E-BP1 complex 10 min after the injection of IRS-1-deficient mice. 4E-BP1 appears as three bands, designated α, β, and γ, representing different extents of phosphorylation (20). Insulin decreased the amounts of the α nonphosphorylated form and the β phosphorylated form with a low stoichiometry and increased the amount of γ, the more highly phosphorylated form, in the muscles of wild-type mice (Fig. 7A, lane c). The effect was less extensive in the muscles of IRS-1-deficient mice (Fig. 7A, lane d). As was previously observed (21), at least one site in 4E-BP1 may be phosphorylated without the loss of eIF-4E binding; thus, 4E-BP1 α and β are the forms found bound to the initiation factor after the complexes are isolated from the extracts by affinity purification with a resin of the cap homolog m^{7}GTP. The eIF-4E from both control and insulin-treated mice quantitatively bound to the resin (Fig. 7B). Insulin markedly (by about 70%) decreased the amount of 4E-BP1 (α plus β) which bound to the resin in the muscles of wild-type mice (Fig. 7C, lane c), while in the muscles of IRS-1-deficient mice, it decreased the amount by only about 40% (Fig. 7C, lane d, and Fig. 7E). After these mice were stimulated with EGF, which stimulates the dissociation of the eIF-4E–4E-BP1 complex via a pathway in-

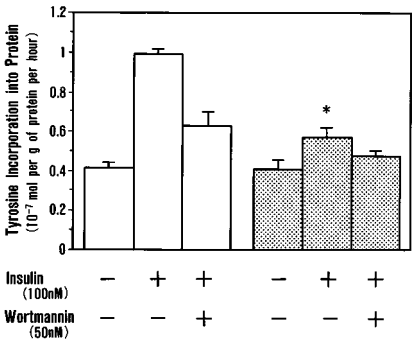

FIG. 8. Effect of insulin on the incorporation of [^{3}H]tyrosine into protein in soleus muscles from wild-type (open bars) and IRS-1-deficient (stippled bars) mice in vitro. Soleus muscles were preincubated for 30 min in Ham's F12 medium and then were incubated with L-[^{3}H]tyrosine for 1 h, and then the tyrosine incorporation into protein was calculated as described in Materials and Methods. Each bar represents the mean ± standard error for muscles from eight to nine mice without wortmannin treatment. *, $P < 0.001$ for insulin-incubated muscles from wild-type mice versus insulin-incubated muscles from IRS-1-deficient mice. In some experiments, muscles were preincubated or not with 50 nM wortmannin for 30 min. The results for muscles treated with wortmannin are the means ± standard errors for more than four separate experiments shown in duplicate.

dependent of IRS-1, the responses were virtually identical (a decrease of about 90%) (Fig. 7C, lanes e and f). The dissociation of eIF-4E and 4E-BP1 was also assessed by determining the amount of eIF-4E that was coimmunoprecipitated with 4E-BP1 antibody (Fig. 7D). Insulin decreased the amount of eIF-4E that was coimmunoprecipitated with 4E-BP1 from the muscles of wild-type and IRS-1-deficient mice by about 70 and 40%, respectively, agreeing well with the findings with m^7GTP-Sepharose. These data suggested that the initiation of translation by insulin stimulation was impaired in the muscles of IRS-1-deficient mice.

Protein synthesis rate in skeletal muscles. Since the initiation of the translation of insulin stimulation was impaired in the muscles of IRS-1-deficient mice, we next measured the protein synthesis rate in soleus muscles of wild-type and IRS-1-deficient mice which were incubated in vitro with insulin for 1 h. Insulin (100 nM) caused a 2.5-fold stimulation of the protein synthesis rate in muscles from wild-type mice, whereas it caused a 1.4-fold stimulation in IRS-1-deficient mice (Fig. 8). When both groups were stimulated with EGF, which stimulates protein synthesis via a pathway independent of IRS-1, the responses were comparable (data not shown). To evaluate whether the upstream pathway of protein synthesis would be wortmannin sensitive, the protein synthesis rate was measured after a pretreatment with 50 nM wortmannin for 30 min. Wortmannin decreased insulin-induced protein synthesis by approximately 50% in muscles from both wild-type and IRS-1-deficient mice (Fig. 8).

PI3-kinase and MAP kinase activities in liver tissue. For an evaluation of the potential differences in insulin signalling among different target organs, we measured PI3-kinase activity in livers from wild-type and IRS-1-deficient mice. Two minutes after insulin injection, there was a maximal increase in kinase activity (Fig. 9A and B). In livers, PI3-kinase activity in PY20 immunoprecipitates was stimulated by about 6.8-fold in wild-type mice and about 5.4-fold in IRS-1-deficient mice (Fig. 9A and B). We also measured MAP kinase activity in the livers and found that 5 min after the insulin injection, MAP kinase activity in αC92 immunoprecipitates was stimulated by about 3.3-fold in wild-type mice and about 2.9-fold in IRS-1-deficient mice (Fig. 9C and D). Thus, the maximal responses for insulin-induced PI3-kinase and MAP kinase activation in livers in IRS-1-deficient mice were slightly but not significantly impaired compared with those in the wild type.

Amount of tyrosine phosphorylation of IRS-1 and IRS-2 in mouse muscles and livers. The molecular causes for the difference in the degrees of insulin resistance for muscles and livers from IRS-1-deficient mice were determined with the phosphotyrosine proteins in the muscles and livers 5 min after insulin injection. We observed a 175-kDa tyrosine-phosphorylated protein (IRS-1) in both the muscles and livers of insulin-injected wild-type mice (Fig. 10A and B, lanes b). In contrast, in IRS-1-deficient mice, there was only a 190-kDa tyrosine-phosphorylated protein (pp190 [IRS-2]) in the two tissues in insulin-injected mice (Fig. 10A and B, lanes d). As can be seen from Fig. 10C and D, the amount of tyrosine-phosphorylated IRS-2 (in IRS-1-deficient mice) was roughly equal to that of IRS-1 (in wild-type mice) in the livers, whereas the tyrosine phosphorylation of IRS-2 was only 20 to 30% of that of IRS-1 in the muscles. The insulin receptor β subunit was tyrosine phosphorylated in an insulin-dependent fashion to similar degrees in IRS-1-deficient mice and wild-type mice in both tissues (Fig. 10A and B, lanes a to d).

With regard to other IRSs, the oncoprotein Shc is tyrosine phosphorylated after being stimulated with insulin. Five minutes after the insulin injection, the tyrosine phosphorylation of Shc in muscles and livers was assessed by immunoblotting with the polyclonal antibody against Shc of PY20 immunoprecipitates. Shc was phosphorylated to similar degrees in IRS-1-deficient mice and wild-type mice in both organs (Fig. 10E). Occasionally, tyrosine phosphorylation of Shc was slightly but not significantly increased in IRS-1-deficient mice in the two tissues. It should be noted that although EGF stimulation resulted in the tyrosine phosphorylation of both the 52- and 46-kDa Shc isoforms, insulin stimulation resulted in the tyrosine phosphorylation of only the former isoform, which was consistent with the previous report (25).

DISCUSSION

To better understand the physiological roles of IRS-1 in vivo, we and others made mice with a targeted disruption of the IRS-1 gene and demonstrated that IRS-1-deficient mice exhibited growth retardation and also had resistance to the glucose-lowering effects of insulin and insulin-like growth factor 1 (1, 36). Furthermore, a 190-kDa tyrosine-phosphorylated protein (pp190/IRS-2) which is functionally and structurally similar to IRS-1 has been presumed to compensate for the function of IRS-1 deficiency, at least in part, in IRS-1 knockout mice. In this study, we investigated the mechanism of insulin resistance by comparing insulin's actions in its target organs, skeletal muscle and liver, in wild-type and IRS-1-deficient mice.

Site of insulin resistance. We showed that the stimulation of 2-DG transport activity with insulin in the isolated soleus muscle was significantly impaired in IRS-1-deficient mice, which was concomitant with a decrease in insulin-induced PI3-kinase activity. These data suggested that impaired glucose transport in skeletal muscles in response to insulin was one mechanism of resistance to the glucose-lowering effects of insulin in IRS-1-deficient mice. In addition, other insulin actions, such as p70 S6 kinase and MAP kinase activation, mRNA translation, and protein synthesis, were severely impaired in the muscles of IRS-1 knockout mice. In contrast to the situation with the muscles, an analysis of insulin action showed that both insulin-induced MAP kinase activation and PI3-kinase activation were

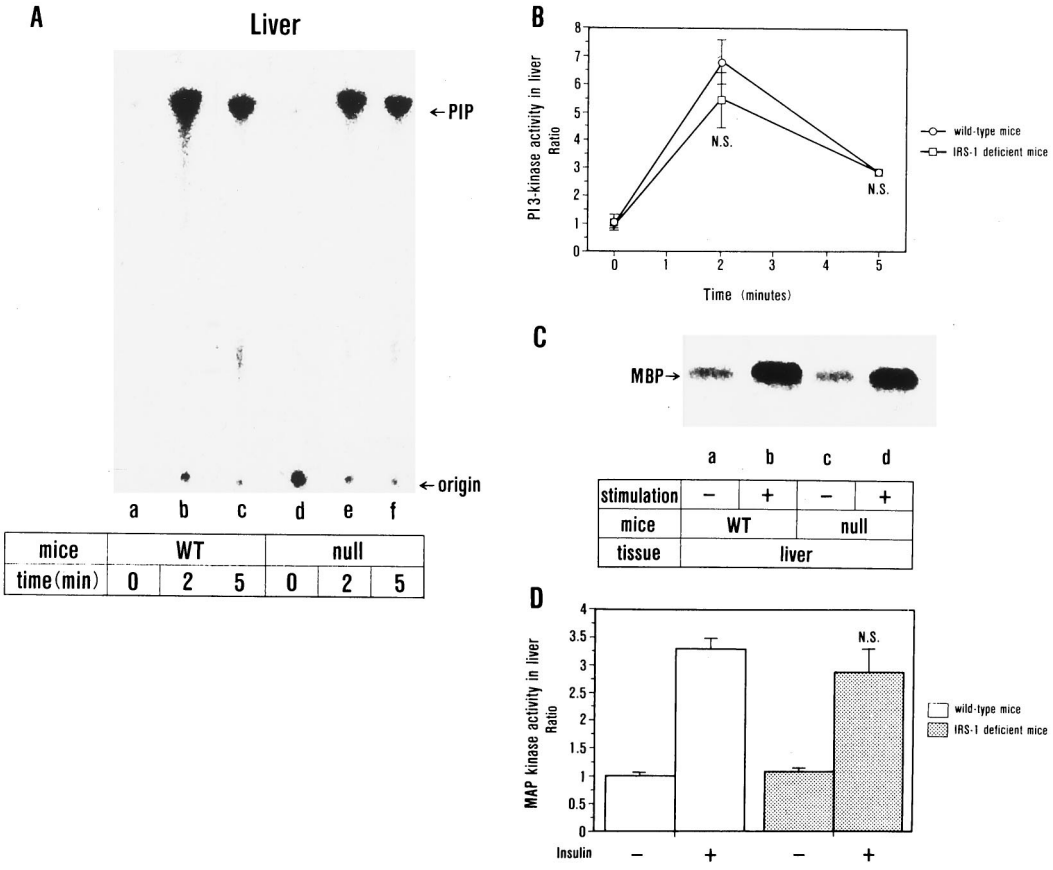

FIG. 9. PI3-kinase and MAP kinase activities in the livers of wild-type (WT) and IRS-1-deficient (null) mice. (A and B) PI3-kinase activity in the immunoprecipitates with anti-phosphotyrosine (PY20) from the livers of wild-type and IRS-1-deficient mice. The anti-phosphotyrosine immunoprecipitates from the liver lysates of untreated (time, 0 min) and insulin-treated wild-type and IRS-1-deficient mice for the indicated periods were subjected to a PI3-kinase assay. The autoradiogram of the thin-layer chromatograph is shown (A). The radioactivity in the spots corresponding to phosphatidylinositol (PIP) was measured, and the results, expressed as the ratios of the values for the respective mice to those for untreated wild-type mice, are shown (B). Each bar represents the mean ± standard error for livers from three to seven mice. N.S., the difference is not significant for insulin-injected wild-type mice versus insulin-injected IRS-1-deficient mice. (C and D) MAP kinase activity in the immunoprecipitates with the antibody against MAP kinase (αC92) from the livers of wild-type and IRS-1-deficient mice. Liver extracts from untreated and insulin-treated wild-type and IRS-1-deficient mice (treatment time, 5 min) were subjected to immunoprecipitation with αC92 and then to a kinase assay toward MBP. Labeled MBP was subjected to SDS-PAGE and then to autoradiography (C). The radioactivity in the bands corresponding to MBP was measured, and the results, expressed as the ratios of the values for the respective mice to those for untreated wild-type mice, are shown (D). Each bar represents the mean ± standard error for livers from three to six mice. N.S., the difference is not significant for insulin-injected wild-type mice versus insulin-injected IRS-1-deficient mice.

comparable in the livers of wild-type and IRS-1-deficient mice. We concluded that the insulin resistance of IRS-1-deficient mice was mainly due to resistance in the muscles.

Compensation of IRS-1 by IRS-2 in IRS-1-deficient mice. We sought to learn the molecular basis for the differences in the impairment of insulin actions in these mice by investigating insulin-stimulated, tyrosine-phosphorylated proteins in the muscles and livers. Interestingly, in the muscles, the amount of tyrosine-phosphorylated IRS-2 (in IRS-1-deficient mice) was much less than that of IRS-1 (in wild-type mice), whereas the amounts in the livers were roughly equal. In addition, the amount of PI3-kinase p85- or Grb2-associated tyrosine-phosphorylated IRS-2 in the muscles was also much less than that of IRS-1. Thus, the degree of compensation for IRS-1 deficiency appeared to be correlated with the amount of tyrosine-phosphorylated IRS-2 (in IRS-1-deficient mice) relative to that of IRS-1 (in wild-type mice). The mechanisms by which the significant induction of tyrosine phosphorylation of IRS-2 in IRS-1-deficient mice and the differences in the relative amounts of tyrosine-phosphorylated IRS-2 for the muscles and livers take place are not known at present. Possible mechanisms may include an altered expression of IRS-2 and an altered efficiency of the tyrosine phosphorylation of IRS-2. These important issues should be addressed in future studies. With regard to other substrates, tyrosine phosphorylation of Shc was either unchanged or occasionally slightly but not significantly increased in both the muscles and livers of IRS-1-deficient mice, suggesting that Shc may not play an important role in compensation for IRS-1 deficiency. We cannot exclude the possibility that molecules other than IRS-2 which we could not detect under our conditions may be involved in compensation for IRS-1 deficiency.

Role of IRS-1 or the IRS-1–IRS-2 system in insulin's action. It is difficult to dissect the roles of IRS-1 in such tissues as liver, in which IRS-1 deficiency is well compensated for by IRS-2. Thus, we analyzed the roles of IRS-1 in muscle tissues, in which tyrosine phosphorylation of IRS-2 is much less than that with liver tissues. We showed that all of the actions of insulin that we studied—insulin-induced PI3-kinase activation, glucose transport, p70 S6 kinase and MAP kinase activation, mRNA translation, and protein synthesis—were impaired in IRS-1-deficient mice, even in the presence of IRS-2 and Shc. We

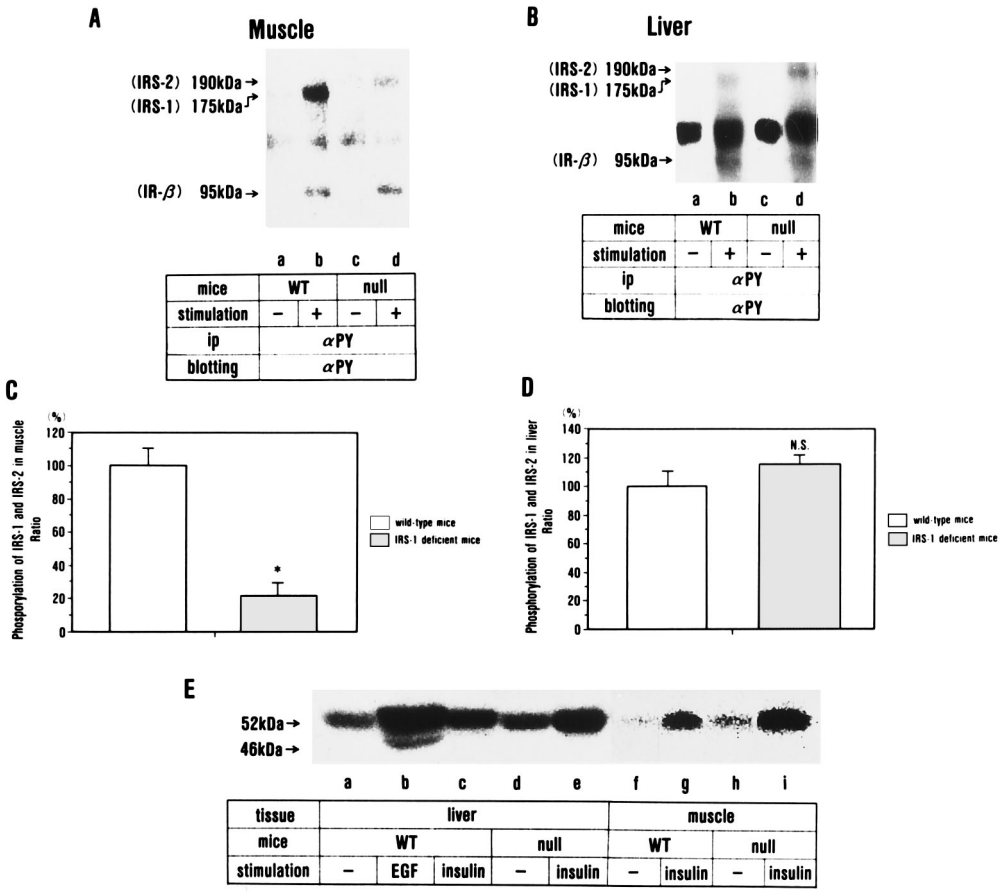

FIG. 10. Insulin-stimulated phosphotyrosine proteins in muscles and livers from wild-type (WT) and IRS-1-deficient (null) mice. (A and B) Phosphotyrosine proteins in mouse muscles (A) and livers (B) 5 min after insulin injection. Wild-type (lanes a and b) and IRS-1-deficient (lanes c and d) mice were not (lanes a and c) or were (lanes b and d) injected with insulin via portal veins. After 5 min, the skeletal muscles from the hind limbs and the livers were removed, homogenized in 1% Nonidet P-40–buffer A (see Materials and Methods), and centrifuged. The supernatants were subjected to immunoprecipitation with anti-phosphotyrosine (αPY [PY20]) and then to Western blotting with the polyclonal anti-phosphotyrosine antibody and then to detection with ^{125}I-protein A. ip, immunoprecipitate; IR-β, insulin receptor β subunit. (C and D) Amount of tyrosine phosphorylation of IRS-1 in wild-type mice and that of IRS-2 in IRS-1-deficient mice in muscles (C) and livers (D). The amount of tyrosine phosphorylation, normalized by the amount of receptor autophosphorylation, was evaluated by densitometry of the autoradiographs and expressed as the percentage of tyrosine phosphorylation of IRS-1 in wild-type mice. Each bar represents the mean ± standard error for more than five independent experiments. *, $P < 0.001$; N.S., the difference is not significant for wild-type mice versus IRS-1-deficient mice. (E) Tyrosine phosphorylation of Shc in mouse livers and muscles 5 min after insulin injection. The PY20 immunoprecipitates from the liver lysates (lanes a to e) and the muscle lysates (lanes f to i) of wild-type (lanes a to c and f and g) and IRS-1-deficient (lanes d, e, h, and i) mice without (lanes a, d, f, and h) and with (lanes c, e, g, and i) insulin and with EGF injection (lane b) were subjected to Western blotting with the polyclonal antibody against Shc and then to detection with ^{125}I-protein A. The results are representative of five separate experiments.

could at least conclude that IRS-1 was necessary for those insulin actions we discussed above.

In particular, the answer to the question of whether IRS-1 has an important function in mediating MAP kinase activation is controversial. In IRS-1-deficient mice, IRS-2 instead of IRS-1 was induced to be tyrosine phosphorylated and to bind Ash/Grb2 by insulin stimulation, and Shc could bind Ash/Grb2 to a similar extent in wild-type mice. The maximal response in insulin-induced MAP kinase activation was nevertheless severely impaired in the muscles of IRS-1-deficient mice compared with that in wild-type mice. These data provided the first evidence that the insulin-stimulated association of Ash/Grb2 with tyrosine-phosphorylated IRS-1 may be a major mechanism for insulin-induced MAP kinase activation in the physiological target organ, skeletal muscles. The partial activation of MAP kinase by insulin may be mediated, at least in part, by tyrosine phosphorylation of IRS-2. In addition, Shc might also be involved in the activation of MAP kinase in combination with IRS-2–Grb2 complexes in IRS-1-deficient mice and with IRS-1–Grb2 and possibly with IRS-2–Grb2 in wild-type mice. The result of MAP kinase activity in the muscles of IRS-1-deficient mice was not consistent with the results with various transformed cell lines. Those results argued for the role of Shc rather than IRS-1 in the activation of MAP kinase by insulin. Furthermore, insulin-stimulated MAP kinase activation was not significantly impaired in the livers of IRS-1-deficient mice, unlike the effect in the muscles. This result may be due to the fact that the amount of tyrosine-phosphorylated IRS-2 (in IRS-1-deficient mice) was roughly equal to that of IRS-1 (in wild-type mice) in the livers whereas the level of tyrosine phosphorylation of IRS-2 was much lower than that of IRS-1 in the muscles (also see Discussion above). The precise pathways used by the insulin receptor to mediate its biological effects may vary among the tissues and cell lines used and may depend on the relative levels of competition among IRS-1, IRS-2, Shc, and other unidentified signalling molecules.

In muscles from IRS-1-deficient mice, the responses to insulin-induced p70 S6 kinase and MAP kinase activation were

severely impaired. Since both p70 S6 kinase and MAP kinase-p90 S6 kinase have been implicated in insulin-stimulated protein synthesis via several mechanisms, we measured insulin-stimulated protein synthesis in the muscles. The rate of protein synthesis stimulated with insulin was severely impaired in muscles from IRS-1-deficient mice. This observation provided the first evidence that IRS-1 plays a pivotal role in protein synthesis stimulated with insulin in the physiological target organ. Under our conditions, 50 nM wortmannin almost completely prevented the increase in p70 S6 kinase activity stimulated by insulin in the muscles, whereas the same dose of wortmannin did not completely but did partially prevent the increase in the protein synthesis rate, which was consistent with both MAP kinase and p70 S6 kinase being involved in the activation of protein synthesis. To further investigate the mechanism for the impairment of insulin-stimulated protein synthesis, we studied the dissociation of the eIF-4E–4E-BP1 complex in muscles. The response was impaired in the muscles of IRS-1-deficient mice, suggesting that decreased phosphorylation of 4E-BP1 by p70 S6 kinase and/or MAP kinase may be one of the mechanisms accounting for the decreased protein synthesis rate in IRS-1-deficient mice.

In conclusion, (i) IRS-1 plays a central role in two major biological actions of insulin, glucose transport and protein synthesis in muscles; (ii) the insulin resistance of IRS-1-deficient mice is mainly due to resistance in the muscles; and (iii) the degree of compensation for IRS-1 deficiency appears to be correlated with the amount of tyrosine-phosphorylated IRS-2 (in IRS-1-deficient mice) relative to that of IRS-1 (in wild-type mice).

ACKNOWLEDGMENTS

We are grateful to Yasuko Murakami (Jikei University of School of Medicine) for helpful suggestions and to Noriko Takahashi, Yasunori Kadowaki, Shoji Asai, Tadashi Yamamoto, Keiji Iwamoto, and Eriko Komaki for technical assistance. We thank Ikuko Kato for typing the manuscript.

This work was supported by grant 192125 from the Juvenile Diabetes Foundation International (to T.K.) and by a grant for diabetes research from the Ohtsuka Pharmaceutical Co., Ltd. (to T.K.).

REFERENCES

1. **Araki, E., M. A. Lipes, M. E. Patti, J. C. Brüning, B. Haag III, R. S. Johnson, and C. R. Kahn.** 1994. Alternative pathway of insulin signalling in mice with targeted disruption of the IRS-1 gene. Nature (London) **372:**186–190.
2. **Backer, J. M., M. G. Myers, Jr., S. E. Shoelson, D. J. Chin, X. J. Sun, M. Miralpeix, P. Hu, B. Margolis, E. Y. Skolnik, J. Schlessinger, and M. F. White.** 1992. Phosphatidylinositol 3′-kinase is activated by association with IRS-1 during insulin stimulation. EMBO J. **11:**3469–3479.
3. **Cheatham, B., C. J. Vlahos, L. Cheatham, L. Wang, J. Blenis, and C. R. Kahn.** 1994. Phosphatidylinositol 3-kinase activation is required for insulin stimulation of pp70 S6 kinase, DNA synthesis, and glucose transporter translocation. Mol. Cell. Biol. **14:**4902–4911.
4. **Chen, D., D. J. Van Horn, M. F. White, and J. M. Backer.** 1995. Insulin receptor substrate 1 rescues insulin action in CHO cells expressing mutant insulin receptors that lack a juxtamembrane NPXY motif. Mol. Cell. Biol. **15:**4711–4717.
5. **Chung, J., T. C. Grammer, K. P. Lemon, A. Kazlauskas, and J. Blenis.** 1994. PDGF- and insulin-dependent pp70^{S6K} activation mediated by phosphatidylinositol-3-OH kinase. Nature (London) **370:**71–75.
6. **Chung, J., C. J. Kuo, G. R. Crabtree, and J. Blenis.** 1992. Rapamycin-FKBP specifically blocks growth-dependent activation of and signaling by the 70 kd S6 protein kinases. Cell **69:**1227–1236.
7. **Fingar, D. C., S. F. Havsdorff, J. Blenis, and M. J. Birnbaum.** 1993. Dissociation of pp70 ribosomal protein S6 kinase from insulin-stimulated glucose transport in 3T3-LI adipocytes. J. Biol. Chem. **268:**3005–3008.
8. **Frayn, K. N., and P. F. Maycock.** 1979. Regulation of protein metabolism by a physiological concentration of insulin in mouse soleus and extensor digitorum longus muscles. Biochem. J. **184:**323–330.
9. **Graves, L. M., K. E. Bornfeldt, G. M. Argast, E. G. Krebs, X. Kong, T. A. Lin, and J. C. J. Lawrence.** 1995. cAMP- and rapamycin-sensitive regulation of the association of eukaryotic initiation factor 4E and the translational regulator PHAS-I in aortic smooth muscle cells. Proc. Natl. Acad. Sci. USA **92:**7222–7226.
10. **Hansen, P. A., E. A. Gulve, and J. O. Holloszy.** 1994. Suitability of 2-deoxyglucose for in vitro measurement of glucose transport activity in skeletal muscle. J. Appl. Physiol. **76:**979–985.
11. **Honda, R. Y., K. Tobe, Y. Kaburagi, K. Ueki, S. Asai, M. Yachi, M. Shirouzu, Y. Akanuma, S. Yokoyama, Y. Yazaki, and T. Kadowaki.** 1995. Upstream mechanisms of glycogen synthase activation by insulin and insulin-like growth factor-1. J. Biol. Chem. **270:**2729–2734.
12. **Jefferson, L. S., K. E. Flaim, and D. E. Peavy.** 1981. Effect of insulin on protein turnover, p. 133–177. *In* M. Brownlee (ed.), Handbook of diabetes mellitus: biochemical pathology, vol. 4. Garland Press, New York.
13. **Jeffries, H. B. J., C. Reinhard, S. C. Kozma, and G. Thomas.** 1994. Rapamycin selectively represses translation of the "polypyrimidine tract" mRNA. Proc. Natl. Acad. Sci. USA **91:**4441–4445.
14. **Kaburagi, Y., R. Y. Honda, K. Tobe, K. Ueki, M. Yachi, Y. Akanuma, R. M. Stephens, D. Kaplan, Y. Yazaki, and T. Kadowaki.** 1995. The role of the NPXY motifs in the insulin receptor in tyrosine phosphorylation of insulin receptor substrate-1 and Shc. Endocrinology **136:**3437–3443.
15. **Kaburagi, Y., K. Momomura, R. Y. Honda, K. Tobe, Y. Tamori, H. Sakura, Y. Akanuma, Y. Yazaki, and T. Kadowaki.** 1993. Site-directed mutagenesis of the juxtamembrane domain of the human insulin receptor. J. Biol. Chem. **268:**16610–16622.
16. **Kadowaki, T., S. Koyasu, E. Nishida, K. Tobe, T. Izumi, F. Takaku, H. Sakai, I. Yahara, and M. Kasuga.** 1987. Tyrosine phosphorylation of common and specific sets of cellular proteins rapidly induced by insulin, insulin-like growth factor I, and epidermal growth factor in an intact cell. J. Biol. Chem. **262:**7342–7350.
17. **Kasuga, M., Y. Fujita-Yamaguchi, D. L. Blithe, and C. R. Kahn.** 1983. Tyrosine-specific protein kinase activity is associated with the purified insulin receptor. Proc. Natl. Acad. Sci. USA **80:**2137–2141.
18. **Lavan, B. E., M. R. Kuhne, C. W. Garner, D. Anderson, M. Reedijk, T. Pawson, and G. E. Lienhard.** 1992. The association of insulin-elicited phosphotyrosine proteins with Src homology 2 domains. J. Biol. Chem. **267:**11631–11636.
19. **Lejbkowicz, F., C. Goyer, A. Darveau, S. Nerson, R. Lemieux, and N. Sonenberg.** 1992. A fraction of the mRNA 5′ cap-binding protein, eukaryotic initiation factor 4E, localizes to the nucleus. Proc. Natl. Acad. Sci. USA **89:**9612–9616.
20. **Lin, T. A., X. Kong, T. A. J. Haystead, A. Pause, G. Belsham, N. Sonenberg, and J. C. J. Lawrence.** 1994. PHAS-I as a link between mitogen-activated protein kinase and translation initiation. Science **266:**653–656.
21. **Lin, T. A., X. Kong, A. R. Saltiel, P. J. Blackshear, and J. C. J. Lawrence.** 1995. Control of PHAS-I by insulin in 3T3-LI adipocytes. J. Biol. Chem. **270:**18531–18538.
22. **Lowry, O. H., N. J. Rosebrough, A. L. Farr, and R. J. Randall.** 1951. Protein measurement with the Folin phenol reagent. J. Biol. Chem. **193:**265–275.
23. **Matsuoka, K., F. Shibasaki, M. Shibata, and T. Takenawa.** 1993. Ash/Grb-2, a SH2/SH3-containing protein, couples to signaling for mitogenesis and cytoskeletal reorganization by EGF and PDGF. EMBO J. **12:**3467–3473.
24. **Myers, M. G., Jr., L.-M. Wang, X. J. Sun, Y. Zhang, L. Yenush, J. Schlessinger, J. H. Pierce, and M. F. White.** 1994. Role of IRS-1–GRB-2 complexes in insulin signaling. Mol. Cell. Biol. **14:**3577–3587.
25. **Okada, S., K. Yamauchi, and J. E. Pessin.** 1995. Shc isoform-specific tyrosine phosphorylation by the insulin and epidermal growth factor receptors. J. Biol. Chem. **270:**20737–20741.
26. **Okada, T., Y. Kawano, T. Sakakibara, O. Hazeki, and M. Ui.** 1994. Essential role of phosphatidylinositol 3-kinase in insulin-induced glucose transport and antilipolysis in rat adipocytes. J. Biol. Chem. **269:**3568–3573.
27. **Patti, M. E., X. J. Sun, J. C. Bruening, E. Araki, M. A. Lipes, M. F. White, and C. R. Kahn.** 1995. 4PS/insulin receptor substrate (IRS)-2 is the alternative substrate of the insulin receptor in IRS-1-deficient mice. J. Biol. Chem. **270:**24670–24673.
28. **Pause, A., G. J. Belsham, A. C. Gingras, O. Donze, T. A. Lin, J. C. J. Lawrence, and N. Sonenberg.** 1994. Insulin-dependent stimulation of protein synthesis by phosphorylation of a regulator of 5′-cap function. Nature (London) **371:**762–767.
29. **Pelicci, G., L. Lanfrancone, F. Grignani, J. McGlade, F. Y. Cavallo, G. Forni, I. Nicoletti, F. Grignani, T. Pawson, and P. G. Pelicci.** 1992. A novel transforming protein (SHC) with an SH2 domain is implicated in mitogenic signal transduction. Cell **70:**93–104.
30. **Price, D. J., J. R. Grove, V. Calvo, J. Avruch, and B. E. Bierer.** 1992. Rapamycin-induced inhibition of the 70-kilodalton S6 protein kinase. Science **257:**973–977.
31. **Pruett, W., Y. Yuan, E. Rose, A. G. Batzer, N. Harada, and E. Y. Skolnik.** 1995. Association between Grb2/Sos and insulin receptor substrate 1 is not sufficient for activation of extracellular signal-regulated kinases by interleukin-4: implications for Ras activation by insulin. Mol. Cell. Biol. **15:**1778–1785.
32. **Sasaoka, T., B. Draznin, J. W. Leitner, W. J. Langlois, and J. M. Olefsky.** 1994. Shc is the predominant signaling molecule coupling insulin receptors to activation of guanine nucleotide releasing factor and p21^{ras}-GTP forma-

tion. J. Biol. Chem. **269:**10734–10738.
33. **Skolnik, E. Y., C. H. Lee, A. G. Batzer, L. M. Vicentini, M. Zhov, R. J. Daly, M. G. Myers, Jr., J. M. Backer, A. Ullrich, M. F. White, and J. Schlessinger.** 1993. The SH2/SH3 domain-containing protein GRB2 interacts with tyrosine-phosphorylated IRS-1 and Shc: implications for insulin control of ras signalling. EMBO J. **12:**1929–1936.
34. **Sun, X. J., P. Rothenberg, C. R. Kahn, J. M. Backer, E. Araki, P. A. Wilden, D. A. Cahill, B. J. Goldstein, and M. F. White.** 1991. The structure of the insulin receptor substrate IRS-1 defines a unique signal transduction protein. Nature (London) **352:**73–77.
35. **Sun, X. J., L. M. Wang, Y. Zhang, L. Yenush, M. G. J. Myers, E. Glasheen, W. S. Lane, J. H. Pierce, and M. F. White.** 1995. Role of IRS-2 in insulin and cytokine signaling. Nature (London) **377:**173–177.
36. **Tamemoto, H., T. Kadowaki, K. Tobe, T. Yagi, H. Sakura, T. Hayakawa, Y. Terauchi, K. Ueki, Y. Kaburagi, S. Satoh, H. Sekihara, S. Yoshioka, H. Horikoshi, Y. Furuta, Y. Ikawa, M. Kasuga, Y. Yazaki, and S. Aizawa.** 1994. Insulin resistance and growth retardation in mice lacking insulin receptor substrate-1. Nature (London) **372:**182–186.
37. **Tobe, K., T. Kadowaki, K. Hara, Y. Gotoh, H. Kosako, S. Matsuda, H. Tamemoto, K. Ueki, Y. Akanuma, E. Nishida, and Y. Yazaki.** 1992. Sequential activation of MAP kinase activator, MAP kinases, and S6 peptide kinase in intact rat liver following insulin injection. J. Biol. Chem. **267:**21089–21097.
38. **Tobe, K., T. Kadowaki, H. Tamemoto, K. Ueki, K. Hara, O. Koshio, K. Momomura, Y. Gotoh, E. Nishida, Y. Akanuma, Y. Yazaki, and M. Kasuga.** 1991. Insulin and 12-O-tetradecanoylphorbol-13-acetate activation of two immunologically distinct myelin basic protein/microtubule-associated protein 2 (MBP/MAP2) kinases via de novo phosphorylation of threonine and tyrosine residues. J. Biol. Chem. **266:**24793–24803.
39. **Tobe, K., O. Koshio, Y. Tashiro-Hashimoto, F. Takaku, Y. Akanuma, and M. Kasuga.** 1990. Immunological detection of phosphotyrosine-containing proteins in rat livers after insulin injection. Diabetes **39:**528–533.
40. **Tobe, K., K. Matsuoka, H. Tamemoto, K. Ueki, Y. Kaburagi, S. Asai, T. Noguchi, M. Matsuda, S. Tanaka, S. Hattori, Y. Fukui, Y. Akanuma, Y. Yazaki, T. Takenawa, and T. Kadowaki.** 1993. Insulin stimulates association of insulin receptor substrate-1 with the protein abundant Src homology/growth factor receptor-bound protein. J. Biol. Chem. **268:**11167–11171.
41. **Tobe, K., H. Tamemoto, T. Yamauchi, S. Aizawa, Y. Yazaki, and T. Kadowaki.** 1995. Identification of a 190-kDa protein as a novel substrate for the insulin receptor kinase functionally similar to insulin receptor substrate-1. J. Biol. Chem. **270:**5698–5701.
42. **Ueki, K., S. Matsuda, K. Tobe, Y. Gotoh, H. Tamemoto, M. Yachi, Y. Akanuma, Y. Yazaki, E. Nishida, and T. Kadowaki.** 1994. Feedback regulation of mitogen-activated protein kinase kinase kinase activity of c-Raf-1 by insulin and phorbol ester stimulation. J. Biol. Chem. **269:**15756–15761.
43. **Wang, L.-M., A. D. Keegan, W. Li, G. E. Lienhard, S. Pacini, J. S. Gutkind, M. G. Myers, Jr., X.-J. Sun, M. F. White, S. A. Aaronson, W. E. Paul, and J. H. Pierce.** 1993. Common elements in interleukin 4 and insulin signaling pathways in factor-dependent hematopoietic cells. Proc. Natl. Acad. Sci. USA **90:**4032–4036.
44. **Wang, L.-M., M. G. Myers, Jr., X.-J. Sun, S. A. Aaronson, M. F. White, and J. H. Pierce.** 1993. IRS-1: essential for insulin- and IL-4-stimulated mitogenesis in hematopoietic cells. Science **261:**1591–1594.
45. **White, M. F., and C. R. Kahn.** 1994. The insulin signaling system. J. Biol. Chem. **268:**1–4.
46. **White, M. F., R. Maron, and C. R. Kahn.** 1985. Insulin rapidly stimulates tyrosine phosphorylation of a Mr-185,000 protein in intact cells. Nature (London) **318:**183–186.
47. **Yamauchi, K., and J. E. Pessin.** 1994. Insulin substrate-1 (IRS-1) and Shc compete for a limited pool of Grb2 in mediating insulin downstream signaling. J. Biol. Chem. **269:**31107–31114.
48. **Yeh, J. I., E. A. Gulve, L. Rameh, and M. J. Birnbaum.** 1995. The effects of wortmannin on rat skeletal muscle. J. Biol. Chem. **270:**2107–2111.
49. **Yonezawa, K., A. Ando, Y. Kaburagi, R. Yamamoto-Honda, T. Kitamura, K. Hara, M. Nakafuku, Y. Okabayashi, T. Kadowaki, Y. Kaziro, and M. Kasuga.** 1994. Signal transduction pathways from insulin receptors to Ras. J. Biol. Chem. **269:**4634–4640.
50. **Yoshizawa, F., A. Tonouchi, Y. Miura, K. Yagasaki, and R. Funabiki.** 1995. Insulin-stimulated polypeptide chain elongation in the soleus muscle of mice. Biosci. Biotechnol. Biochem. **59:**348–349.